LAWRENCE
LIVERMORE
NATIONAL
LABORATORY

UCRL-TR-217950

Aging and Phase Stability of Alloy 22 Welds

FY04 SUMMARY REPORT

Bassem El-Dasher [1],Sharon G. Torres , Michael McGregor, and Tammy S. Edgecumbe

Yucca Mountain Project
Lawrence Livermore National Laboratory

Nancy Yang, Thomas Headley, Jeff Chames, Ja Lee Yio, and Andy Gardea

Department of Analytical Material Science (8773)
Sandia National Laboratories, CA

January 3, 2006

[1] Corresponding author: eldasher2@llnl.gov

Auspices
This work was performed under the auspices of the U.S. Department of Energy by University of California, Lawrence Livermore National Laboratory under Contract W-7405-Eng-48.

TABLE OF CONTENTS

Executive Summary

The work presented in this report consists of a compilation of individual activity reports sent to BSC at the conclusion of the FY04 fiscal year. A chapter is dedicated for each individual activity, and describes the accomplishments at the time of writing the original reports, and includes experimental data when appropriate. It is important to note that since work for most of the activities was intended for completion in FY05, no DTN numbers are given in the present report and the results presented here are to be considered preliminary at the time of their writing. Information and results presented in the FY05 Summary Report (UCRL-TR-217339) are more comprehensive and complete and supersede those given in the present report.

The accomplishments for the five activities addressed in this report are summarized below.

1. Preliminary Evaluation of Burnished and Peened Samples - Metallurgy

- Received 4 each (12 total) of as-welded, burnished, and peened bars. The 12 as received bars were cut into 6 pieces per bar; 15 pieces (22 mm x 6 mm x 25 mm) were used for aging and metallographic sample preparation. The remaining 60 pieces (most of which are only base metal) are being stored.
- Aging was performed on twelve of the specimens (4 for each stress mitigation condition). Three additional specimens (one for each as-fabricated condition) were prepared for analyses, but were not aged. The fifteen specimens were prepared metallographically for Scanning Electron Microscope (SEM) imaging and Electron Back Scatter Diffraction (EBSD) analyses to identify and quantify the phases observed in the (SEM).
- Q-training for six persons at Sandia National Laboratory was completed.
- Microhardness measurements performed on as-welded, burnished, and peened specimens in the as-fabricated condition.
- Development of methodology for Transmission Electron Microscopy (TEM) sample preparation and quantification of long-range ordering (LRO) analyses began in June 2004. TEM sample preparation completed on the as-welded (non-aged), burnished, and peened specimens aged at 550°C for 1000 hours (4 total). TEM analyses was started in September 2004 and stopped September 30, 2004 (end of the fiscal year). Work to resume in FY05.
- 182 SEM images taken of the 3 specimens in the as-received condition for bulk volume fraction measurements. 83 images were taken of the specimens aged at 700°C for 50 and 500 hours (P and μ phases) using EBSD and analyzed using a preliminary automated method of measuring volume fraction with Image Pro Plus. This method still needs to be validated with the manual technique for statistical accuracy.

2. Preliminary Heat-to-Heat Variability Study – Metallurgical

- 98 welded plates were received from Allegheny Ludlum in June 2004.
- Discrepancies were identified in trying to determine which compositions/heats went with which plates. Weld filler metal used was 686 not Alloy 22. Additional documentation requested and received from the BSC Design group (Doug Smith) in September, 2004.
- Six metallurgical samples were cut from each plate at Aqua Jet, with a total number of samples of 588. Analyses of plates to proceed upon resolution of traceability documentation concern.

3. Evaluation of FY00 Mockup Samples - Metallurgy

- A total of 43 machined cylindrical samples and the solution annealed quarter-length, full-diameter prototype waste package were received.
- Transverse sections from the seam weld specimen and the trunnion weld specimen were cut for metallographic preparation for observation in the Scanning Electron Microscope.
- To obtain an estimate of total volume fraction of Topologically Close-Packed (TCP) phases in each specimen, the top of the weld regions across the entire width (~30 mm for the trunnion weld and 21 mm for the seam weld by a 4 mm depth) of both specimens were imaged and analyzed. A total of 223 images were taken.
- A preliminary methodology was developed to automate the measurement of the images used for volume fraction to increase the efficiency of the process so that a greater number of images could be measured in a shorter period of time (an order of magnitude faster).
- Comparisons between manually making volume fraction measurements are being made to ensure accuracy between the two methods.
- Sample preparation was done for Electron Backscatter Diffraction (EBSD) analyses to identify and quantify the phases observed in the Scanning Electron Microscope.

4. Weld Stability with Thick Prototypical Welds

- 52 gas tungsten arc-welded (GTAW) prototypical plates produced at Framatome under the direction of BSC/ACD have been received.
- Weld stability test matrix was finalized in June 2004.
- Samples for testing were cut by water jet. For Topological Close-Pack (TCP) studies: 15 samples for tensile tests (600°C) and 40 samples for metallurgical characterization; for Long-Range Ordering (LRO) studies: 129 samples for tensile tests and 49 samples for metallurgical characterization.
- Sample blanks were introduced into the low and high temperature aging facility furnaces in October 2004 and will be removed from furnaces based on the test matrices.

5. Effect of Solution Annealing on Weld Metallurgy

- High temperature thermocouples and readout were procured and calibrated to perform 1200°C and 1300°C solution anneals.
- Sixteen (25 mm x 6 mm x 25 mm) weld specimens were water jet cut from a Framatome weld plate (762 mm x 203 mm x 32 mm) cleaned, engraved, and aged at four different temperatures and times.
- Thirty prisms with welds were tested in environments using cyclic polarization corrosion tests in the as-welded and aged conditions. All specimens were ground with 600 grit paper prior to testing.
- Five of the sixteen solution anneal specimens were prepared metallographically for Scanning Electron Microscope (SEM) imaging and Electron Back Scatter Diffraction (EBSD) analyses.
- EBSD maps were completed on as-welded specimens, aged at 1075°C for 20 minutes, 24 hours, 72 hours, and 1 week, and also at 1121°C for 20 minutes. The imaging for volume fraction measurements is on-going.

1. Preliminary Evaluation of Burnished and Peened Samples - Metallurgy (AWPT28)

1.1. Objective

To evaluate the effect of controlled plasticity burnishing and laser shock peening on the microstructure, phase stability, and mechanical properties of stress mitigated Alloy 22 welds.

1.2. Accomplishments/Status

- Received 4 each (12 total) of as-welded, burnished, and peened bars as shown in Figure 1.2.1 (305 mm x 13 mm x 25 mm) in April 2004.

Figure 1.2.1. Top and bottom images of as-welded, burnished, and peened bars received for stress mitigation studies.

- The 12 as received bars were cut into 6 pieces per bar; 15 pieces (22 mm x 6 mm x 25 mm) were used for aging and metallographic sample preparation. The remaining 60 pieces (most of which are only base metal) are being stored.
- Specimens were marked and documentation performed to ensure sample traceability.
- Aging conditions performed for twelve of the specimens are shown in Table 1.2.1. Three additional specimens (one for each as-fabricated condition) were prepared for analyses, but were not aged.

Table 1.2.1. Test matrix for stress mitigated Alloy 22 welded plate.

Stress Mitigation Process	Temperature (°C)	Time (hrs.)	Completed
None (as-welded)	None	None	**X**
Low Plasticity Burnishing	None	None	**X**
Laser Shock Peening	None	None	**X**
None (as-welded)	700	50	**X**
Low Plasticity Burnishing	700	50	**X**
Laser Shock Peening	700	50	**X**
None (as-welded)	550	100	**X**
Low Plasticity Burnishing	550	100	**X**
Laser Shock Peening	550	100	**X**
None (as-welded)	700	500	**X**
Low Plasticity Burnishing	700	500	**X**
Laser Shock Peening	700	500	**X**
None (as-welded)	550	1000	**X**
Low Plasticity Burnishing	550	1000	**X**
Laser Shock Peening	550	1000	**X**

- Fifteen specimens were prepared metallographically for Scanning Electron Microscope (SEM) imaging and Electron Back Scatter Diffraction (EBSD) analyses to identify and quantify the phases observed in the (SEM).
- Q-training for six persons at Sandia National Laboratory completed in June 2004.
- Microhardness measurements performed on as-welded, burnished, and peened specimens in the as-fabricated condition. Traces were done transversely across the top of the weld and along the weld centerline for all three samples (~15-30 measurements made per trace in 100μ increments across the top of the weld and 500μ to 1 mm increments longitudinally).
- Development of methodology for Transmission Electron Microscopy (TEM) sample preparation and quantification of long-range ordering (LRO) analyses began in June 2004.
- TEM sample preparation started on the as-welded (non-aged), burnished, and peened specimens aged at 550°C for 1000 hours (4 total) in July 2004 and completed in August 2004.
- TEM analysis was started in September 2004 and stopped September 30, 2004 (end of the fiscal year). Work to resume in FY05.
- 182 SEM images taken of the 3 specimens in the as-received condition for bulk volume fraction measurements using Image Pro Plus.

- 83 images were taken of the specimens aged at 700°C for 50 and 500 hours (P and μ phases) using EBSD and analyzed using a "preliminary" automated method of measuring volume fraction with Image Pro Plus. This method still needs to be validated with the manual technique for statistical accuracy.

1.3. Discussion

One specimen from each plate was characterized in the as-fabricated condition to use as a comparison for the specimens that would be aged as shown in Table 1. The specimens aged at 700°C were aimed at determining the precipitation rate of Topologically Close-Packed (TCP) phases. The specimens aged at 550°C were aimed at precipitating the ordered phase since long-range ordering occurs below 600°C.

Figures 1.3.1, 1.3.2, and 1.3.3 show the microstructure of the as-welded, laser shock peened, and burnished specimens, respectively. In Figure 1.3.2, the slip lines induced from the deformation by the peening process are evident by the "hatch" lines and the bright white spots are the TCP phase. Note the small dendrite arm spacing at the surface where the peening was done, compared to the center of the weld. The evidence of deformation induced slip lines can also be observed in the burnished sample in Figure 1.3.3 however, to a lesser extent.

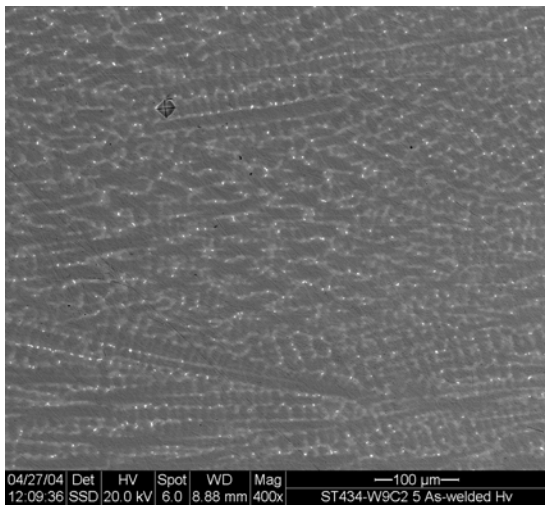

Figure 1.3.1. SEM image showing the microstructure of the as-welded Alloy 22 plate (*i.e.* without stress mitigation).

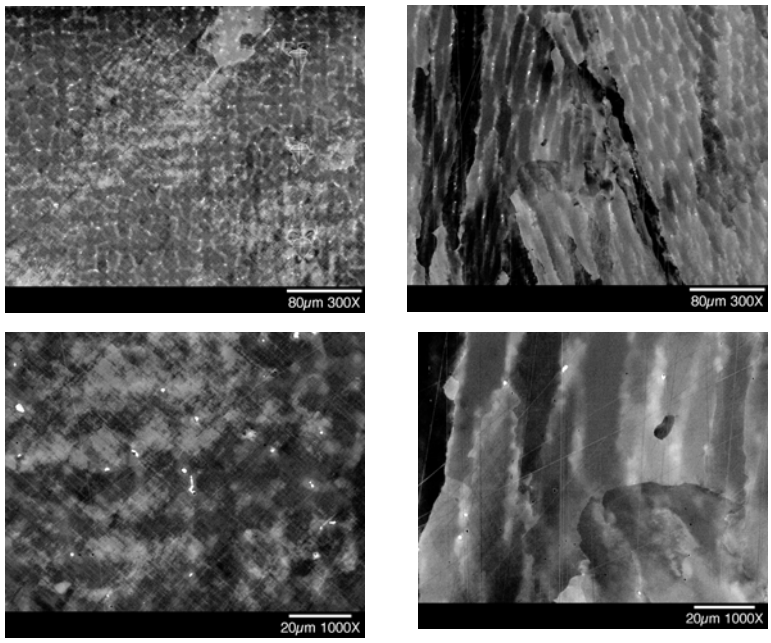

a) Laser Peened (Surface < 1.0 mm) b) Center of Laser Peened Weld

Figure 1.3.2. a) SEM images showing the weld microstructure less than 1 mm from the surface of the laser shock peened Alloy 22 plate. b) SEM images showing the microstructure in the center of the weld ~12 mm below the surface where the microstructure was unaffected by the peening process.

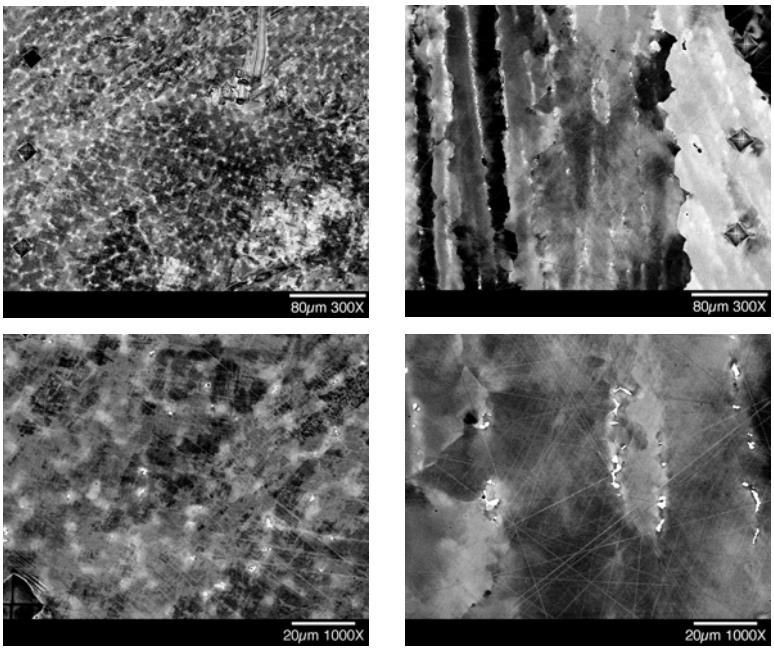

a) Burnished Treated Surface b) Center of Burnished Weld

Figure 1.3.3. a) SEM images showing the weld microstructure of the burnished specimen. b) SEM images showing the microstructure in the center of the weld ~12 mm below the surface where the microstructure was unaffected by the burnishing process.

1.4. Results

1.4.1. Microhardess Evaluation of Stress Mitigated Specimens

Based on the microhardness measurements shown in Figure 1.4.1.1, it can be seen that the burnished sample is harder than the laser peened sample at the surface of the weld in the as received condition. Measurements were taken longitudinally until the measurements leveled off to the value of the as-welded material that had not been subjected to any stress mitigation process. The microhardness measurements also indicate that the deformation induced by the burnishing process was deeper than that of laser peening. The burnishing hardness values did not reach those of the as-welded condition until ~4 mm from the top of the weld, whereas the laser peened hardness values reached the as-welded value at ~2.5 mm.

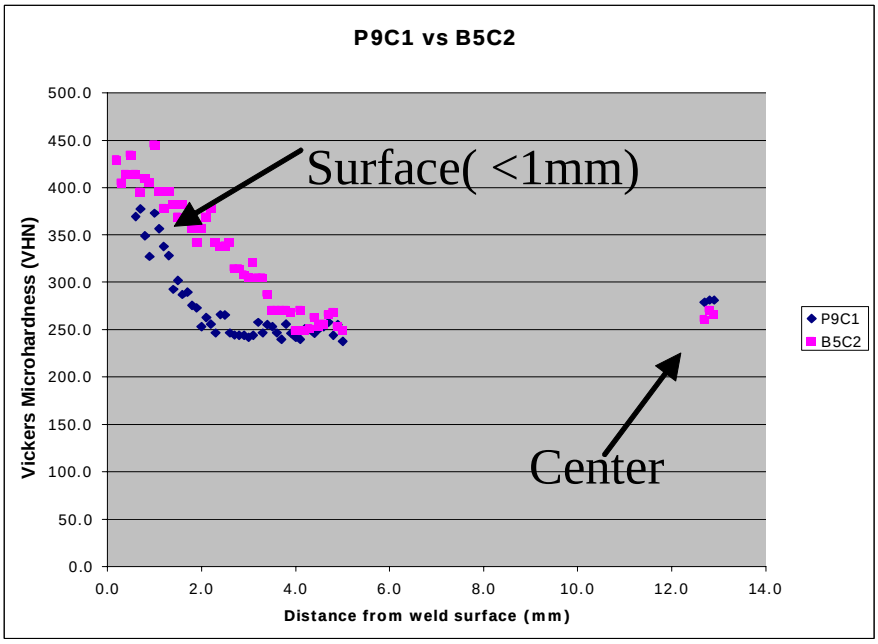

Figure 1.4.1.1. Vickers microhardness measurements for the burnished and peened as-received specimens (without aging).

1.4.2. TCP Phase Identification (Specimens Aged at 700°C)

- Due to the small size of the precipitates in these specimens, automated phase identification using EBSD was not feasible.
- Precipitates were located manually and at random throughout the specimens, and electron diffraction was obtained by manually placing the beam on each precipitate.
- Not all precipitates produced a clear diffraction pattern. For those that did, they were imaged and numbered, and their diffraction patterns were captured and indexed to identify the crystallography as shown in Figure 1.4.2.1.

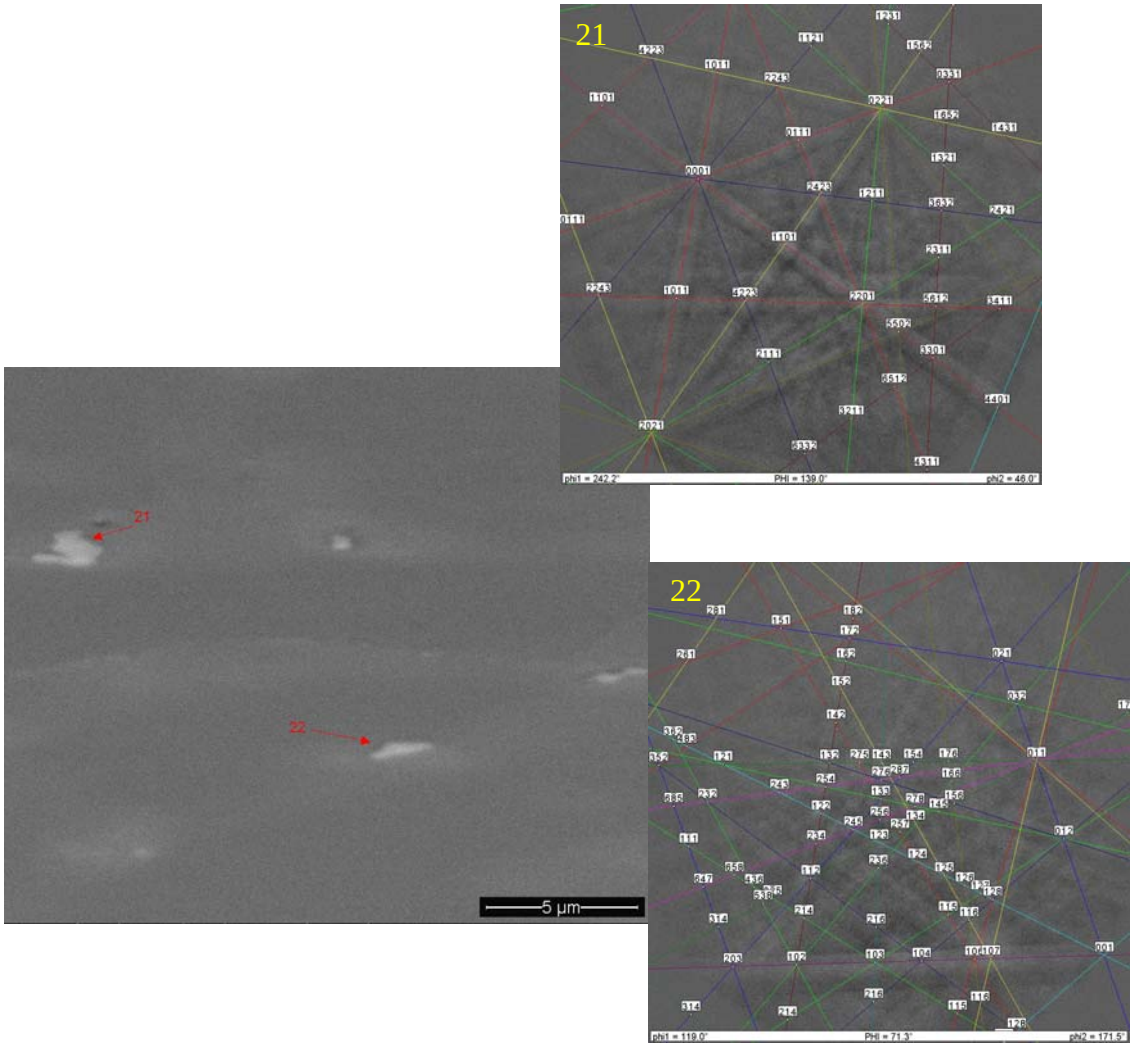

Figure 1.4.2.1. A typical SEM image labeled with the precipitate numbers (red) and their respective captured patterns. Precipitate 21 was indexed as μ, and precipitate 22 as P. Note that the other precipitates in the micrograph did not produce diffraction patterns, and were counted as "unidentified" in the analysis.

- The number of images and precipitates analyzed are listed in Table 1.4.2.1. Table 1.4.2.2 contains the results from the "preliminary" automated use of image analysis used to determine the volume fractions for each individual precipitate, including those that were unidentified.

Table 1.4.2.1. The number of images analyzed and precipitates identified per specimen

Stress Mitigation Treatment	Aging Time @700°C (hr)	# Images	# Precipitates
None	50	15	30
None	500	12	25
Burnished	50	15	30
Burnished	500	12	30
Peened	50	16	30
Peened	500	13	30

Table 1.4.2.2. Relative volume fraction measurements of both identified and unidentified precipitates

Stress Mitigation Treatment	Aging Time @ 700°C (hr)	TCP Phase Fraction (%)			
		P	μ	σ	Unidentified
None	50	49.3	22.8	0.00	27.9
None	500	37.7	27.0	0.00	35.3
Burnished	50	51.5	17.1	0.00	31.3
Burnished	500	47.8	1.7	0.00	50.5
Peened	50	59.5	9.9	0.00	30.6
Peened	500	51.4	8.5	0.00	40.0

- The ratios between the different phases are to be used to weight the total TCP volume fraction, and the percentage unidentified is to be used as a measure of uncertainty.

- The vast majority of identified precipitates were P phase, and typically comprised nearly 50% of the diffracting TCP phases. This result correlates well with the stability of the P phase at the aging temperature of 700°C.

- None of the diffraction patterns captured belonged to a σ-phase precipitate. This is most likely due to the stability of σ-phase at temperatures higher than that used in this study.

1.4.3. LRO Phase Identification (Specimens Aged at 550°C for 1000 hours):

In Figure 1.4.3.1 the fundamental differences in the microstructures among the four samples between the as-welded, welded and aged, peened and aged, and burnished and aged are shown. All the aged samples contain a fine microstructure that is a mix of dislocations and the ordered phase. Additionally, the burnished sample contained a high density of twins (possibly deformation twins). The cause of the observed twinning is yet to be determined.

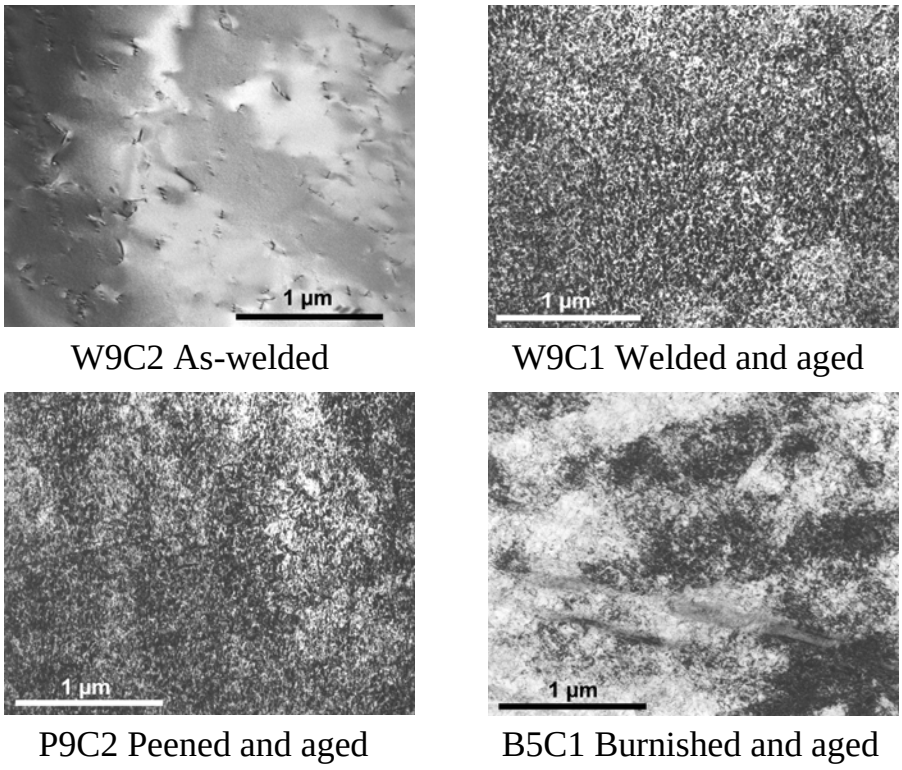

Figure 1.4.3.1. TEM images showing the matrix differences in the as-welded (non-aged) microstructure, and the as-welded, peened and burnished microstructures aged at 550°C for 1000 hours ([110] zone axis). Note the apparent presence of micro-twins in the burnished specimen.

The TEM image shown in Figure 1.4.3.2 shows the presence of dislocations in the as-welded sample however, the selected area electron diffraction (SAED) pattern shows there is no long-range ordering due to the absence of any superlattice reflections.

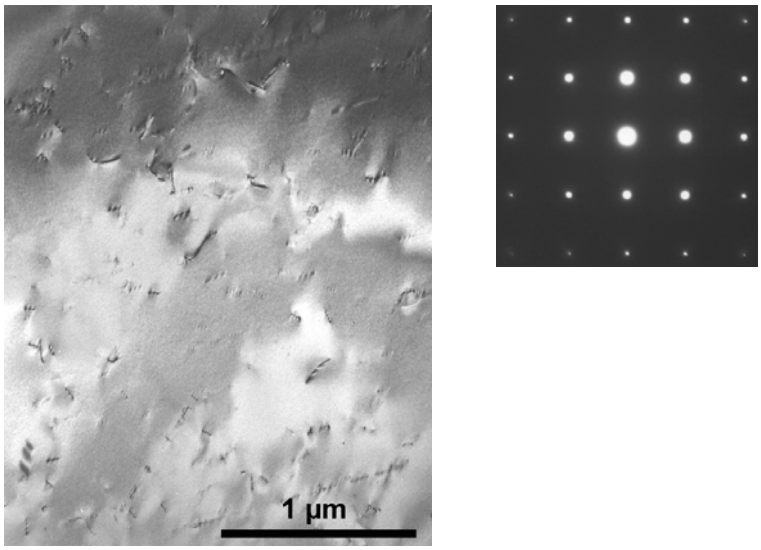

Figure 1.4.3.2. As-welded; bright-field image of matrix (~1.3 mm from the top of the weld) showing dislocations (left) and [001] SAED pattern showing no superlattice reflections indicating no LRO precipitates (right)

The as-welded specimen aged at 550°C for 1000 hours contains nano-scale microstructure features which are dislocations and the ordered phase (see Figure 1.4.3.3). The ordered phase precipitates were verified by the presence of the superlattice reflection pattern in the (SAED) and the precipitates can be seen in the dark field image. The superlattice reflections are uniform in intensity meaning that there are random orientations. TEM specimens were taken 1.45 mm from the top of the weld.

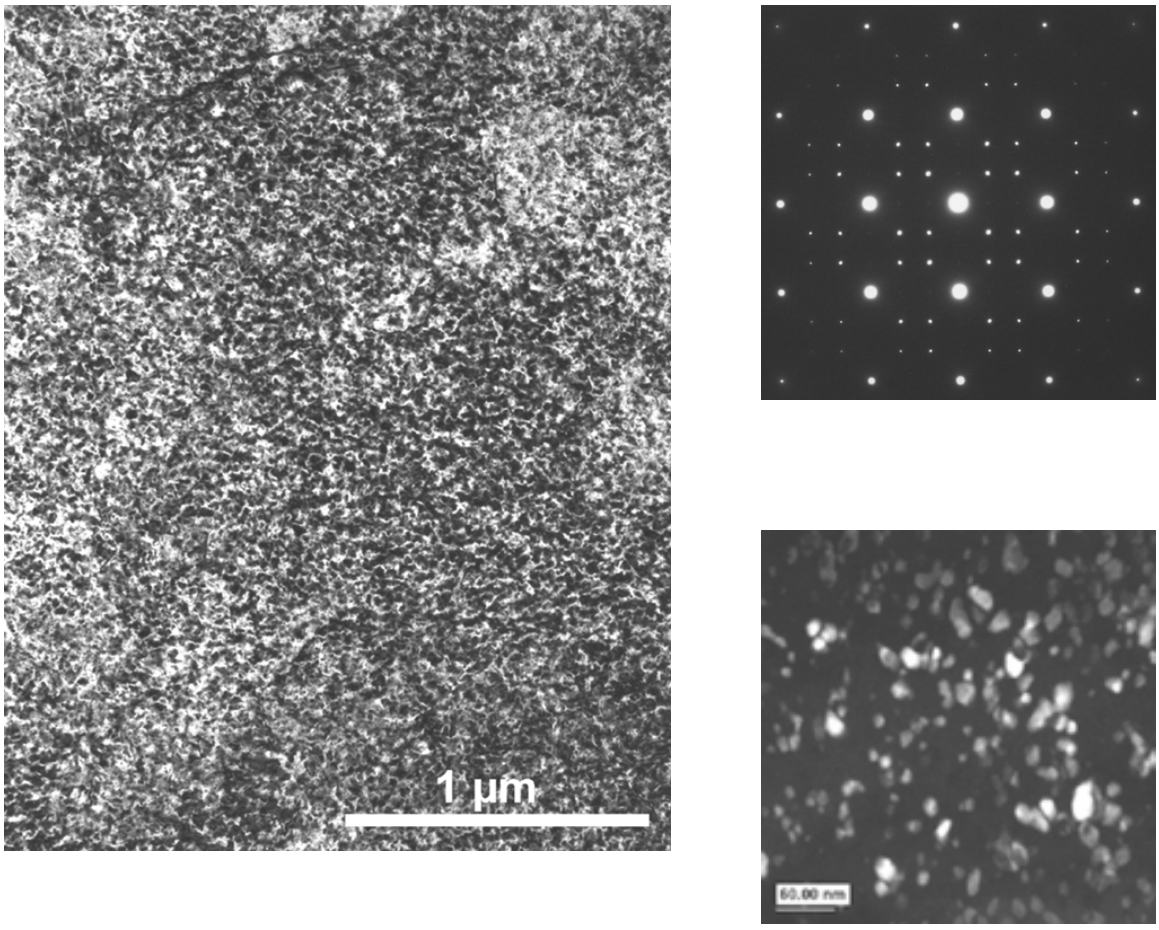

Figure 1.4.3.3. As-welded aged at 550°C for 1000 hours: Bright field image of matrix shows the fine complex features of precipitates/dislocations (left). [001] SAED pattern with LRO superlattice reflections (upper right). Dark field image of LRO phase, one variant, the LRO ~10-30 nm (lower right).

In Figure 1.4.3.4 of the SAED pattern, the two “brighter” diagonal spots of the superlattice reflections indicate possible preferred orientation compared to the as-welded and as-welded aged samples. These TEM specimens were taken 1.5 mm from the top of the weld.

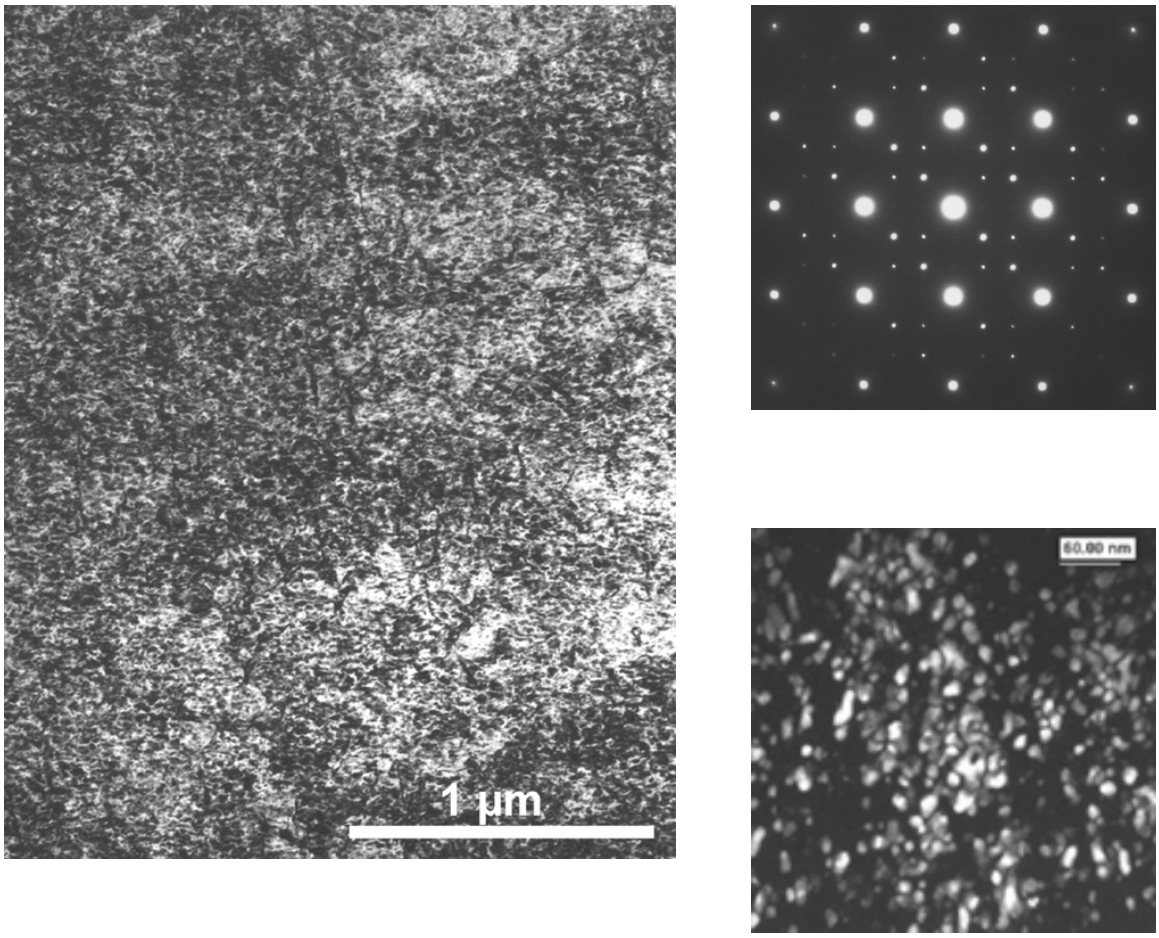

Figure 1.4.3.4. Laser peened specimen aged at 550°C for 1000 hours. Bright field image (left), [001] SAED pattern showing LRO superlattice reflections (upper right). Dark field image of LRO phase, one variant (lower right).

The bright-field image of the matrix for the burnished sample aged at 550°C for 1000 hours contains a non-uniform fine microstructure and twins (due to deformation). All three aged samples contain a high fraction of the ordered phase. The TEM specimens were taken 1.2 mm from the top of the weld. (See Figure 1.4.3.5).

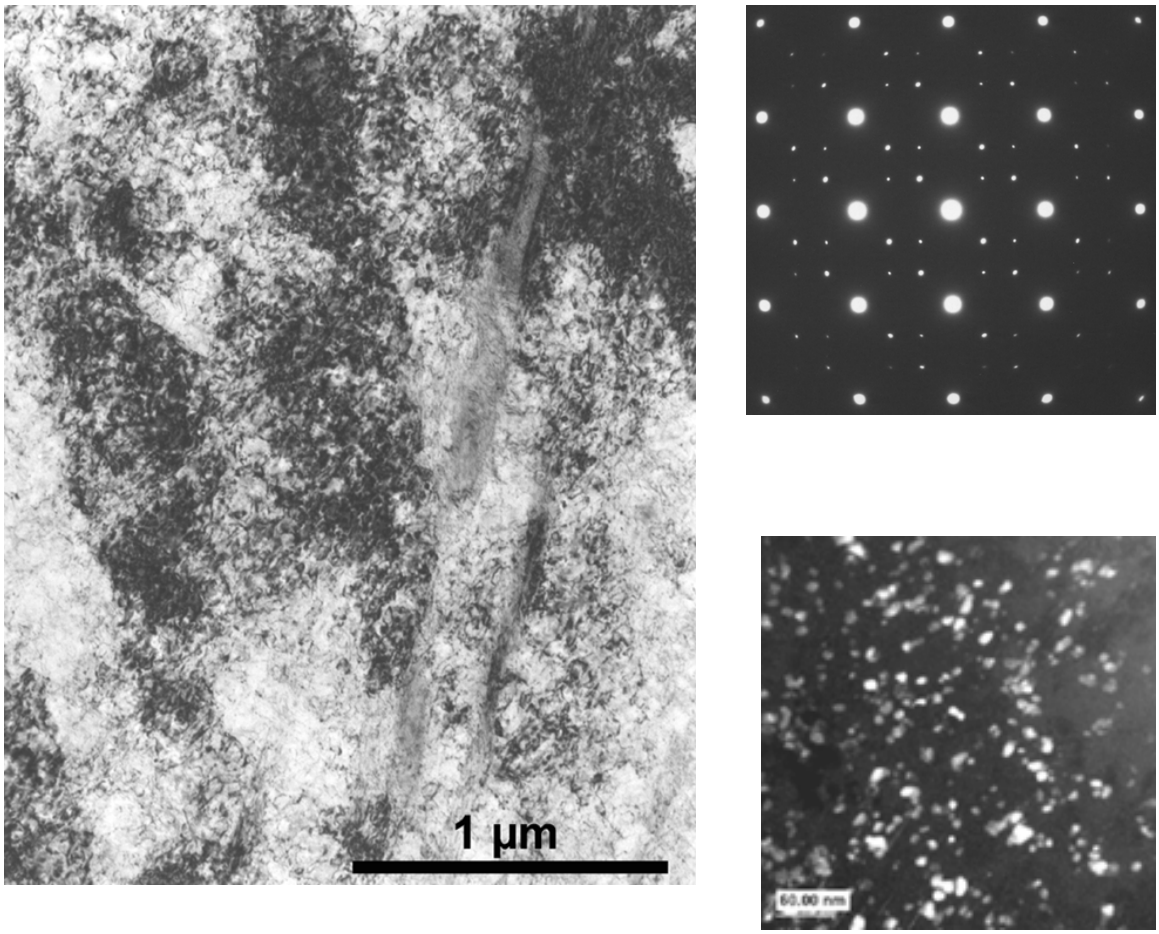

Figure 1.4.3.5. Burnished specimen aged at 550°C for 1000 hours. Bright field image (left). [001] SAED pattern showing LRO superlattice reflections (upper right). Dark field image of LRO phase, one variant (lower right)

From this microstructure, it may be inferred that the increase in hardness in the burnished sample may be due to mechanical deformation introduced by twinning (more boundaries and higher degree of deformation). Microtwinning is evident by the “narrow” band widths (less than 1 micron). From comparison of the SAED patterns, the mechanically treated samples appear to have the superlattice reflections with intensity variation indicating that there may be preferential orientation.

INTENTIONALLY LEFT BLANK

2. Preliminary Heat-to-Heat Variability Study – Metallurgical (AWPT29)

2.1. Objective

To determine the effect of compositional variation from heat-to-heat on the phase stability in Alloy 22 base metal and Alloy 686 weld wire used for welded plates from Gas Tungsten Arc Welding (GTAW).

2.2. Accomplishments/Status

- 98 welded plates (254mm x 203mm x 32mm) were received from Allegheny Ludlum in June 2004.
- Discrepancies were identified in trying to determine which compositions/heats went with which plates.
- Weld filler metal used was 686 not Alloy 22.
- Additional documentation requested and received from the BSC Design group (Doug Smith) in September, 2004.
- Six (13mm x 203mm x 32mm) metallurgical samples were cut from each plate at Aqua Jet in July and August, 2004; total number of samples is 588.
- Metallurgical analyses of plates to proceed upon resolution of traceability documentation concern.

2.3. Discussion

Because heat-to-heat changes in chemical composition are most likely to produce metallurgical changes before any significant changes in corrosion or mechanical properties, results from this study would be used as input to the phase stability thermodynamic model to provide a strong basis for future specifications on composition.

- Plate Welding Parameters:
    - 7 base metal heats and 7 weld wire heats (49 filler metal/base metal combinations)
    - 2 pairs of 48 inch-long bars were welded together (butt weld configuration)
    - Double-U-Groove joint weld geometry with no root opening was utilized to improve weld joint consistency, resulting in a more uniform and repeatable weld
    - Full-thickness along ~ 46 inches of the 48 inch weld joint with 3 filler passes per side
    - Cold-wire feed GTAW process

Table 2.3.1 shows the compositions of base metal and weld filler material that was received from Allegheny Ludlum. Four elements are highlighted in red representing the key elements that can have an effect on the formation of secondary phases such as mu, P, and sigma. All heats are within the acceptable range of the B575 specification for Alloy 22 plate (UNS #N06022) and for Alloy 686 (UNS #N06686) wire. The distinguishing differences between the alloys are the broader range of chromium and the higher molybdenum and tungsten content.

Table 2.3.1. Base metal and weld wire compositions for heat-to-heat studies.

Heat Number	Type	Al	C	Cr	Cu	Fe	Mg	Mo	Ni	O	P	S	V	W
HC70	Wire	0.15	0.004	19.34	0.01	<.02	0.0023	15.10	61.94	0.0015	<.003	<.0003	<.01	3.16
HC71	Wire	0.16	0.005	19.79	0.01	0.42	0.0032	15.75	60.35	0.0011	0.006	<.0003	<.01	3.47
HC72	Wire	0.17	0.002	20.50	0.01	0.39	0.0017	16.25	58.84	0.0010	0.007	<.0003	<.01	3.74
HC73	Wire	0.18	0.001	21.58	0.01	0.28	0.0018	16.25	57.84	0.0013	0.008	<.0003	<.01	3.79
HC74	Wire	0.16	0.001	22.29	0.01	0.35	0.0016	16.28	56.79	0.0011	0.008	<.0003	<.01	4.04
HC75	Wire	0.16	0.002	22.86	0.01	0.14	0.0027	16.82	55.59	0.0012	0.01	<.0003	<.01	4.33
HD15	Wire	0.16	0.005	20.59	0.43	4.03	0.0017	16.26	53.58	<.0006	<.003	<.0004	0.11	3.82
HC76	Plate	0.17	0.003	20.31	0.01	2.51	0.0011	12.71	61.60	0.0015	0.003	<.0003	<.01	2.64
HC77	Plate	0.19	0.004	20.22	0.01	2.50	0.0023	12.63	61.57	<.00065	0.003	<.0003	<.01	2.66
HC78	Plate	0.17	0.005	20.78	<.01	3.00	0.002	13.28	59.67	0.0014	0.004	<.0003	<.01	3.00
HC79	Plate	0.14	0.004	20.81	0.01	3.02	0.0017	13.31	59.59	0.0013	0.004	<.0003	<.01	3.01
HC80	Plate	0.18	0.006	21.22	<.01	3.99	0.0018	13.11	58.39	0.0012	0.004	<.0003	<.01	3.01
HC81	Plate	0.16	0.005	21.03	<.01	3.98	0.0018	13.13	58.64	0.0014	<.003	<.0003	<.01	2.98
HC82	Plate	0.19	0.008	21.60	<.01	4.97	0.0021	13.73	56.37	0.0012	0.006	<.0006	0.01	3.00
HC83	Plate	0.15	0.010	21.60	<.01	5.07	0.0023	13.71	56.33	0.0010	0.006	<.0003	0.01	2.99
HC86	Plate	0.21	0.006	22.36	<.01	5.74	0.0015	14.23	53.95	0.0008	0.006	<.0003	0.01	3.39
HC87	Plate	0.18	0.007	22.39	<.01	5.78	0.0015	14.23	53.90	0.0011	0.006	<.0003	0.01	3.36
HD16	Remake	0.16	0.006	21.22	0.04	3.02	0.0014	13.51	56.03	0.0013	<.003	<.0003	0.25	3.00
HD17	Remake	0.15	0.005	21.31	0.01	2.98	0.0016	13.60	56.00	0.0008	<.003	<.0003	0.25	2.99
B575 Spec.	N06022	-	0.015*	20.0-22.5	-	2.0 - 6.0	0.5*	12.5-14.5	balance		0.02*	0.02*	0.35*	2.5 - 3.5
	N06686		0.01*	19.0-23.0		2.0*		15.0-17.0	balance		0.04*	0.02*		3.0 - 4.4
NOTES:	11 major elements and 15 trace elements measured; values shown above are averages for top and bottom reroll billet samples.													
	For HC70 Ta was .04; all other heats had none measured.													
	*max													
	N06022 is for the plate and N06686 is for the wire.													

- Test Matrix of 98 plates x 6 aging conditions (plus as-fabricated conditions):
  - High temperature sigma: 870°C for 5 min. and 1 hour
  - P and μ phase: 700°C for 50 and 500 hours
  - Long range ordering: 550°C for 100 and 1000 hours
  - As-fabricated/solution annealed @ 1121°C for 30 minutes (one sample from each plate will be analyzed then used for one of the aging conditions).

3. Evaluation of FY00 Mockup Samples - Metallurgy (AWPT30)

3.1. Objective

To evaluate the phase stability of the welds, the heat affected zone (HAZ), and the base metal of a solution annealed quarter-length, full-diameter prototype waste package under the trunnion and away from the trunnion. Cross sectional samples will be examined and any precipitation of secondary phases will be quantified.

3.2. Accomplishments/Status

- A total of 43 machined cylindrical samples (~51 mm x 25 – 51 mm) and the solution annealed quarter-length, full-diameter prototype waste package were received in April 2004. Samples listed below were received from the various areas of the waste package with no post solution anneal oxide film. Visual examination of the waste package indicates that the film has been removed.

    - 15 samples were from the bottom lid
    - 15 samples from the top lid
    - 7 from the longitudinal weld side
    - 4 from the trunnion
    - 2 from the vent hole

- The schematics in Figure 3.2.1 illustrate the transverse sections (sections A for the seam weld specimen, and B for the trunnion weld specimen) that were cut for metallographic preparation for observation in the Scanning Electron Microscope (SEM).

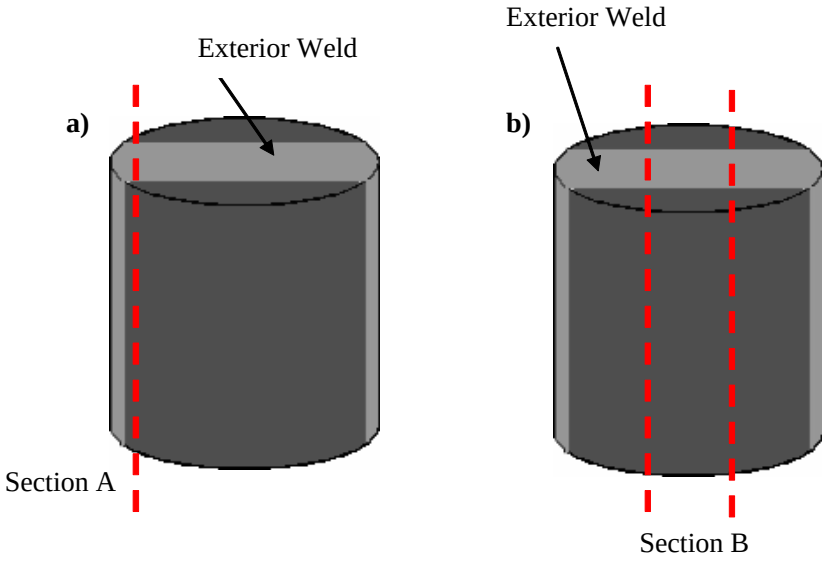

Figure 3.2.1. Schematic illustrating hockey puck sections observed for a) the hockey puck obtained from the seam weld region and b) the hockey puck obtained at the trunnion weld region.

- To obtain an estimate of total volume fraction of Topologically Close-Packed (TCP) phases in each specimen, the top of the weld regions across the entire width (~30 mm for the trunnion weld and 21 mm for the seam weld by a 4 mm depth) of both specimens were imaged and analyzed. A total of 223 images were taken.
- A preliminary methodology was developed to automate the measurement of the images used for volume fraction to increase the efficiency of the process so that a greater number of images could be measured in a shorter period of time (an order of magnitude faster).
- Comparisons between manually making volume fraction measurements are being made to ensure accuracy between the two methods.
- Sample preparation was done for Electron Backscatter Diffraction (EBSD) analyses to identify and quantify the phases observed in the Scanning Electron Microscope (SEM).

3.3. Results

- Using the preliminary automated method of analyses it was observed that although both the trunnion and seam welds have an extremely small volume fraction of precipitates, the trunnion weld had about twice the amount of secondary phase content than the longitudinal seam weld, however, both were less than 0.1%. Both specimens contained weld porosity (which was not measured) formed by gas entrapment during solidification from the welding process.

.

Table 3.3.1. TCP volume fraction for the seam and trunnion welds

Specimen Description	# Images Analyzed	TCP Vol. Fraction (%)
Trunnion Weld	79	<0.1
Seam Weld	144	<0.1

- For the trunnion weld, the majority of the precipitate volume fraction was observed at the exterior of the weld surface as shown in Figure 3.3.1.

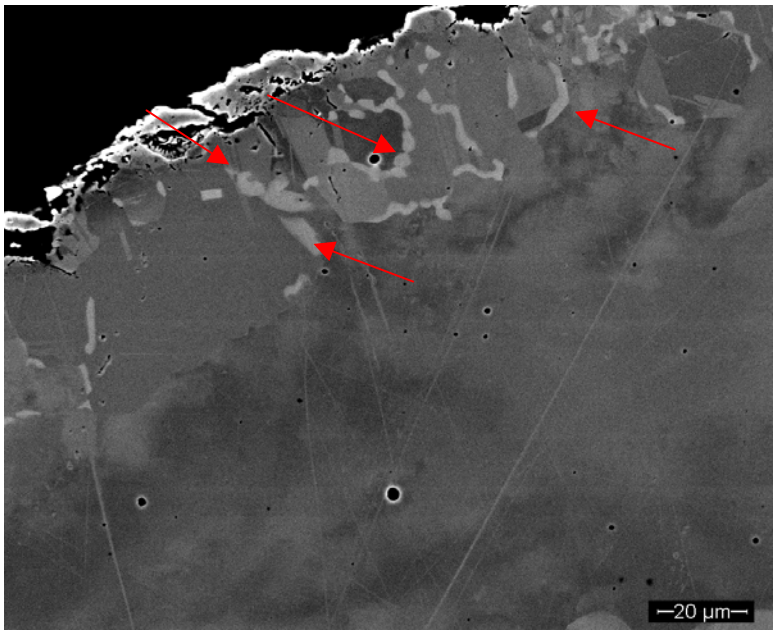

Figure 3.3.1. SEM micrograph showing the coarse precipitation present at the surface of the trunnion weld, as indicated by the red arrows.

- Typically observed precipitation is shown in Figures 3.3.2 and 3.3.3 for the trunnion and seam weld respectively. Note the weld porosity in both specimens.

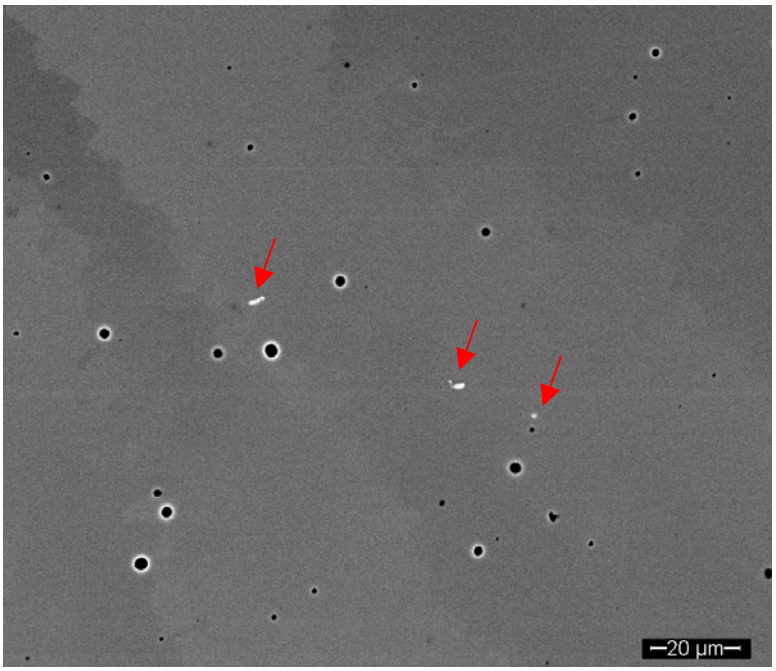

Figure 3.3.2. SEM micrograph showing observed precipitation present in the trunnion closure weld, indicated by the red arrows. Note the presence of a large amount of weld porosity.

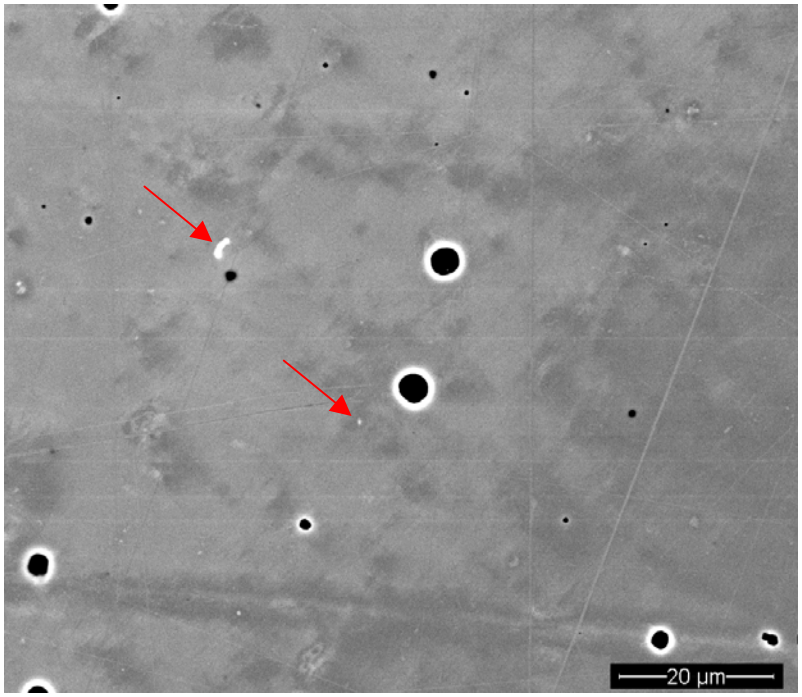

Figure 3.3.3. SEM micrograph showing observed secondary phase precipitation present in the seam weld, indicated by the red arrows. Again note the presence of a large amount of weld porosity.

3.4. Summary

- Trunnion weld had twice the amount of Topologically Close-Packed (TCP) phases than the longitudinal seam weld, however, both were<0.1%.
- Both welds contained weld porosity formed by gas entrapment during solidification from the welding process.
- Coarse precipitation present at the surface of the trunnion weld as shown in Figure 3.3.1 was determined to be the sigma phase.
- The acceptable level of accuracy for the automated method of measuring volume fraction compared to the manual method needs to be determined.

4. Weld Stability with Thick Prototypical Welds (AWPT44)

4.1. Objective

To verify the phase stability of thick (32 mm) prototypical welds (plate) to provide a greater technical basis for the current weld stability model by measuring mechanical properties and precipitate volume fraction as a function of aging time.

4.2. Accomplishments/Status

- 52 gas tungsten arc-welded (GTAW) prototypical plates produced at Framatome under the direction of BSC/ACD have been received.
- Weld stability test matrix was finalized in June 2004.
- Samples for testing were cut by water jet. For Topological Close-Pack (TCP) studies: 15 samples for tensile tests (600°C) and 40 samples for metallurgical characterization; for Long-Range Ordering (LRO) studies: 129 samples for tensile tests and 49 samples for metallurgical characterization.
- Sample blanks were introduced into the low and high temperature aging facility furnaces in October 2004 and will be removed from furnaces based on the test matrixes shown in the next section (Tables 4.3.1 and 4.3.2). Figure 4.2.1 shows the high temperature aging facility, there are two additional furnaces operating at 200 and 300°C.

Figure 4.2.1. High Temperature Aging and Salt Bath Facility for heat treating Alloy 22 base metal and welds.

Figure 4.2.2. Inside View of Furnace with Samples for Aging.

4.3. Discussion

Both the Nuclear Regulatory Commission (NRC) and the Nuclear Waste Technical Review Board (NWTRB) have expressed concern over the effect of heat input during welding of thick sections on metallurgy and corrosion resistance of welds and the heat-affected zone. Verifying the phase stability of thick welds is necessary to provide a greater technical basis for the current model. Thicker welds, such as those planned for the waste package, will require more heat input to the material as a result of the welding process; more heat may alter the initial state of phase precipitation in the welds and therefore the stability of the weld microstructure.

- Plate Welding Parameters:
  - Double-U weld joint geometry was utilized
  - Inconel Filler Metal 622
  - No post-weld heat treatment

Test matrices for TCP and LRO aging studies on thick section Alloy 22 welds are shown in Tables 4.3.1 and 4.3.2.

Table 4.3.1. Test Matrix for Long-Range Ordering (LRO) Aging Studies of Thick (1.25") Welds.

Test Matrix for Aging Studies of Thick Prototypical Alloy 22 Welds to Determine LRO Kinetics																
						Aging Time (Hours)							Aging Time (Years)			
Temp °C	Extras in Furnace	Extra sets out	6 mo. Stagger	1-yr Stagger	2-yr Stagger	5	10	50	100	1000	5000	10k	1	5	10	20
550	2x	2x				x	x	x	x	x						
		2T				T	T	T								
500	2x	2x	x							x	x	x				
		2T	T							T	T	T				
450	2x	2x	x								x	x				
	2T	2T	T								T	T				
400	2x		2x	2x									x	x	x	
	2T		2T	2T									T	T	T	
300	6x														x	x
	6T														T	T
200	6x														x	x
	6T														T	T

Table 4.3.2 Test Matrix for Topologically Close-Pack (TCP) Phase Aging Studies of Thick (32 mm) Welds.

Test Matrix for Aging Studies of Thick Prototypical Alloy 22 Welds to Determine TCP Kinetics												
						Aging Time (hours)						
Temp °C	Extras in Furnace	Extra sets out	6 mo. Stagger	1-yr Stagger	2-yr Stagger	1	10	20	100	1000	10000	50000
750	2x	4x				x	x		x	x		
700	2x	4x					x		x	x	x	
650	2x	2x	2x					x	x	x	x	
600		2x	2x	2x	1x					x	x	x
	Extra samples required at 600°C as both ordering and TCP phase precipitation occur											

INTENTIONALLY LEFT BLANK

5. Effect of Solution Annealing on Weld Metallurgy (AWPT45)

5.1. Objective

To understand the effect of solution annealing on Alloy 22 welds on the precipitate volume fraction and the repassivation potential for crevice corrosion.

5.2. Accomplishments/Status

- High temperature thermocouples (Type R) and readout were procured and calibrated to perform 1200°C and 1300°C solution anneals.
- Sixteen (25 mm x 6 mm x 25 mm) weld specimens were water jet cut from a Framatome weld plate (762 mm x 203 mm x 32 mm) cleaned, engraved, and aged at four different temperatures and times as shown in the solution annealing test matrix (Table 5.3.1).
- Thirty prisms (19 mm x 19 mm x 10 mm) with welds were tested in the environments shown in the cyclic polarization corrosion test matrix (Table 5.3.2) in as-welded and aged conditions. All specimens were ground with 600 grit paper prior to testing.
- Five of the sixteen solution anneal specimens were prepared metallographically for Scanning Electron Microscope (SEM) imaging and Electron Back Scatter Diffraction (EBSD) analyses.
- EBSD maps were completed on as-welded specimens, aged at 1075°C for 20 minutes, 24 hours, 72 hours, and 1 week, and also at 1121°C for 20 minutes (Figures 5.4.1.1 and 5.4.1.2). The imaging for volume fraction measurements is on-going.

5.3. Discussion

Recently, the Center for Nuclear Waste Regulatory Analyses (CNWRA) showed that solution annealing of Alloy 22 welds decreases the repassivation potential for crevice corrosion as compared to as-welded material. The CNWRA tests were conducted with aged samples (870°C for 5 minutes) and tested at temperatures ranging from 60° to 95°C in NaCl solutions with chloride concentrations ranging from 0.001 to 5 M. The tests conducted in this task are designed to show the effect of solution annealing on precipitate volume fraction for short times that are comparable to the baseline solution anneal specified for waste package fabrication. Longer times than the baseline specification have been included in order to clearly demonstrate whether the precipitates, which are known to be present in the as-welded condition, are dissolving or growing during the solution annealing process. Tests using longer times will be used to determine if the precipitates are thermodynamically stable or not.

The testing matrix of solution annealing times and temperatures is shown in Table 5.3.1.

Table 5.3.1. Test Matrix: Solution Annealing Times and Temperatures

Temperature (°C)	Time (hr)			
	0.33	24	96	168
1075	●	●	●	●
1121	●	●	●	●
1200	●	●	•	●
1300	●	●	●	●

Table 5.3.2. shows the test matrix for the cyclic polarization tests that were done on the welded prisms. Based on critical potential tests completed to date, the lower nitrate and intermediate temperature NaCl-KNO_3 environments are most likely to be sensitive to material susceptibility. Cyclic polarization tests were performed according to ASTM G61-86 (Standard Test Method for Conducting Cyclic Potentiodynamic Polarization Measurements for Localized Corrosion Susceptibility of Iron-, Nickel-, or Cobalt-Based Alloys), reversing the scan at the specified current density or one volt, whichever occurs first.

Table 5.3.2. Test Matrix for Cyclic Polarization Corrosion Tests

Environment	Test Temperature (°C)	Number of Specimens per Test	Solution Anneal Conditions
1 Molar NaCl	90	3	None (as-welded)
1 Molar NaCl	90	3	1075°C for 20 min
1 Molar NaCl	90	3	1121°C for 20 min
1 Molar NaCl	90	3	1200°C for 20 min
1 Molar NaCl	90	3	1300°C for 20 min
6 molal NaCl, 0.9 m KNO_3	100	3	None (as-welded)
6 molal NaCl, 0.9 m KNO_3	100	3	1075°C for 20 min
6 molal NaCl, 0.9 m KNO_3	100	3	1121°C for 20 min
6 molal NaCl, 0.9 m KNO_3	100	3	1200°C for 20 min
6 molal NaCl, 0.9 m KNO_3	100	3	1300°C for 20 min

5.4. Results

5.4.1. Microstructural Characterization

- Specimens that were solution annealed were characterized using large scale EBSD mapping.

- Figure 5.4.1.1 provides a graphic illustration of the effects of annealing time on the microstructure. The colors in the figure illustrate the crystallographic plane normals for the grains.

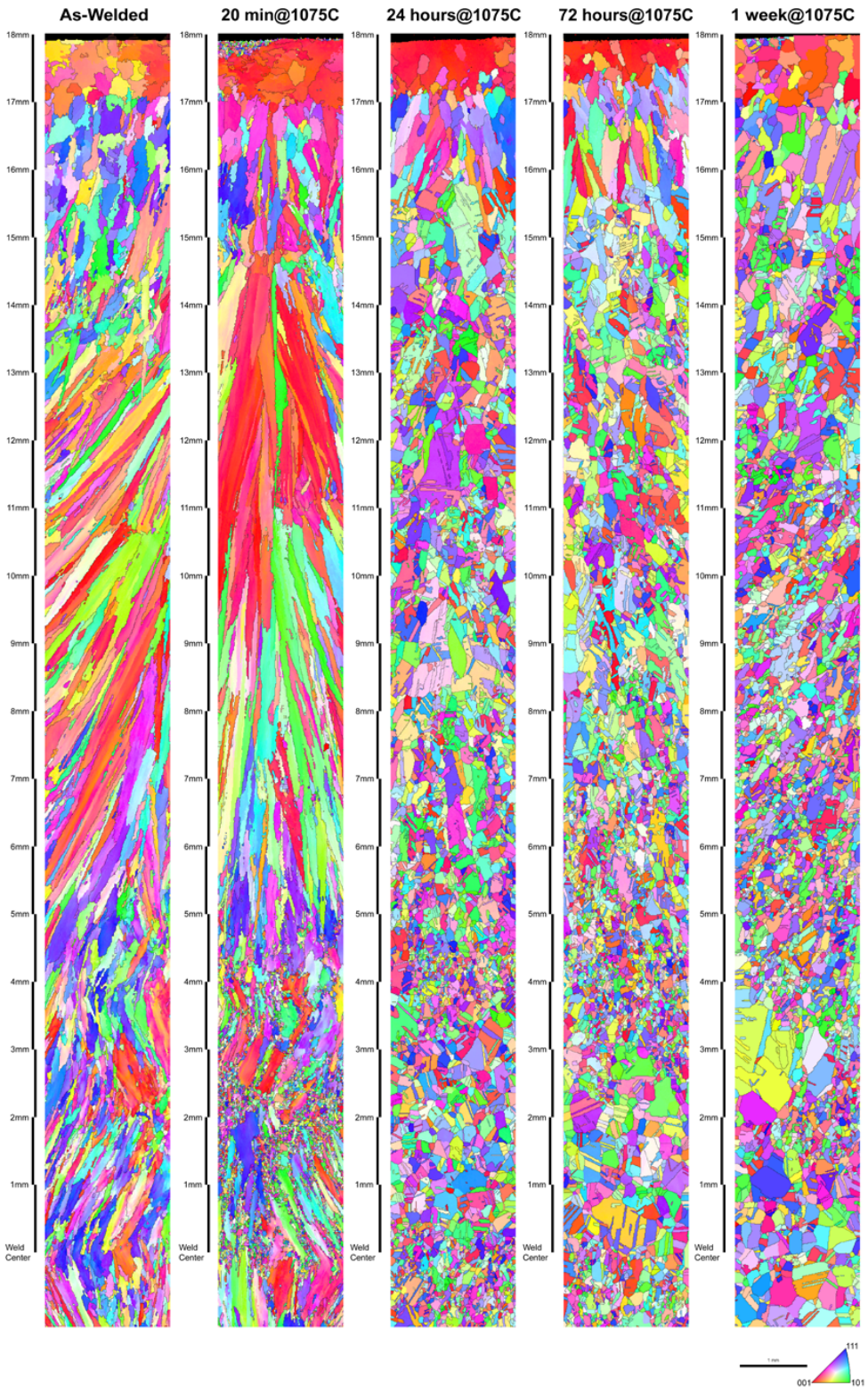

Figure 5.4.1.1. Large scale EBSD maps illustrating the microstructural evolution during solution annealing for various times at 1075^{o}C compared to as-welded microstructure.

- Figure 5.4.1.2 shows a comparison between specimens aged for 20 minutes at 1075°C and 1121°C. Recrystallization occurs faster in the 1121°C sample.

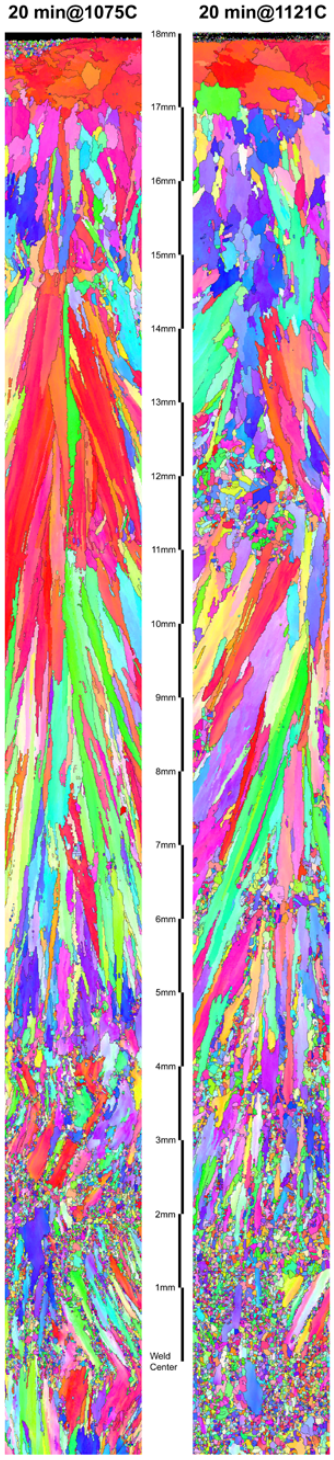

Figure 5.4.1.2. Large scale EBSD maps for welds annealed at 1075°C and 1121°C for 20 minutes showing the rate of recrystallization are faster in the 1121°C specimen.

- The EBSD maps for 1075°C and 1121°C for 20 minutes indicate that the microstructure near the weld surface does not change appreciably for these temperatures and durations. The SEM images of both the as-welded (a) and solution annealed (b) specimen (20 minutes at 1121°C) taken at the top of the weld, as shown in Figure 5.4.1.3 also indicate that annealing for 20 minutes at 1121°C would not necessarily cause the dissolution of Topologically Close-Packed (TCP) phases.

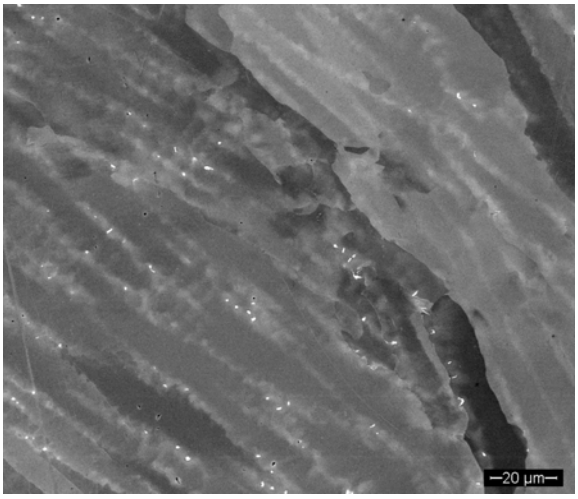

(a)

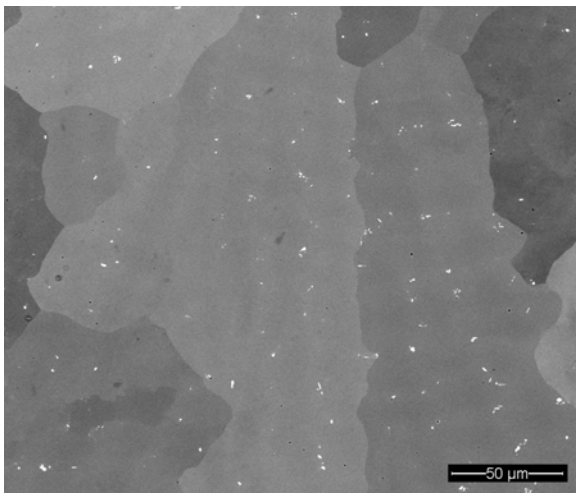

(b)

Figure 5.4.1.3. TCP phases observed near the weld surface in (a) the as-welded specimen and (b) solution annealed for 20 minutes at 1121°C.

5.4.2. Corrosion (Cyclic Polarization) Tests

- Figures 5.4.2.1 and 5.4.2.2 show the cyclic polarization curves for the specimens tested in 1 M NaCl at 90°C and 6 m NaCl + 0.9 m KNO_3 at 100°C, respectively. Crevice corrosion was observed on all test specimens to some degree. In both environments, the amount of hysteresis decreases as annealing temperature increases, indicating higher resistance to localized corrosion for the specimens annealed at higher temperatures. This agrees well with post-test specimen observations (see Figure 5.4.2.3).

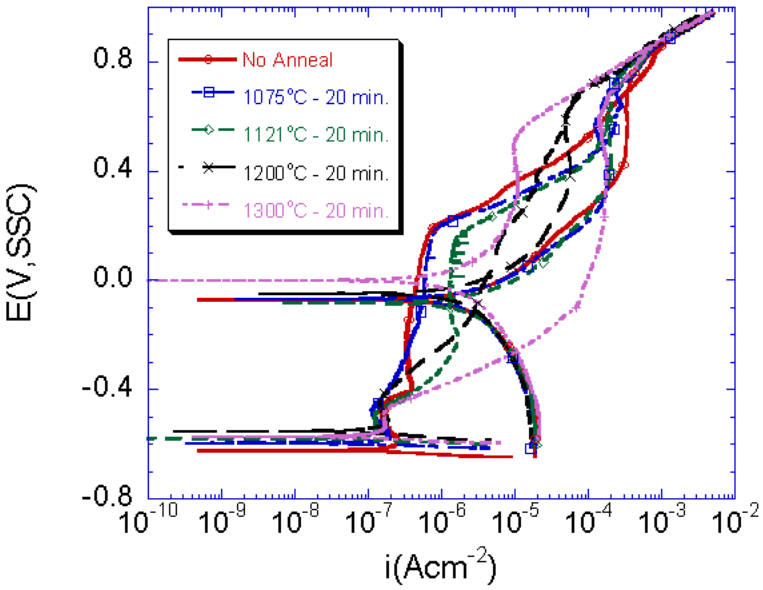

Figure 5.4.2.1. Cyclic polarization curves for 20 minute solution annealing temperature in 1M NaCl at 90°C.

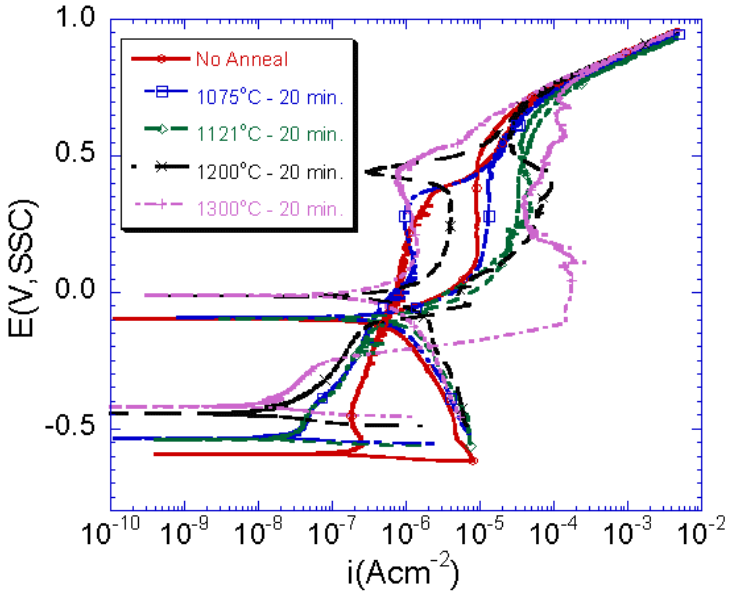

Figure 5.4.2.2. Cyclic polarization curves for 20 minute solution annealing temperature in 6 m NaCl + 0.9 m KNO_3 at 100°C.

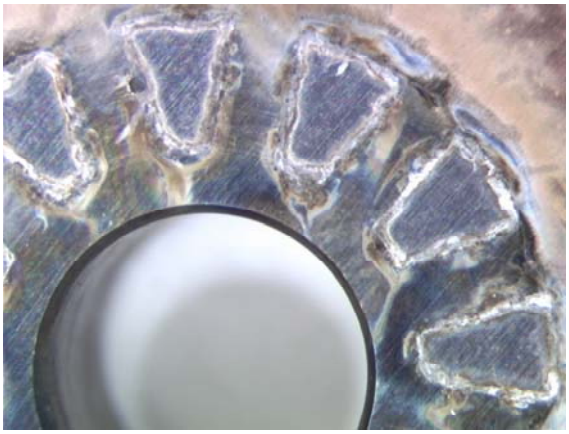

a) Specimen KE0413, non-annealed, tested in 1 M NaCl at 90°C.

b) Specimen KE0490, solution annealed at 1300°C for 20 minutes, tested in 1 M NaCl at 90°C

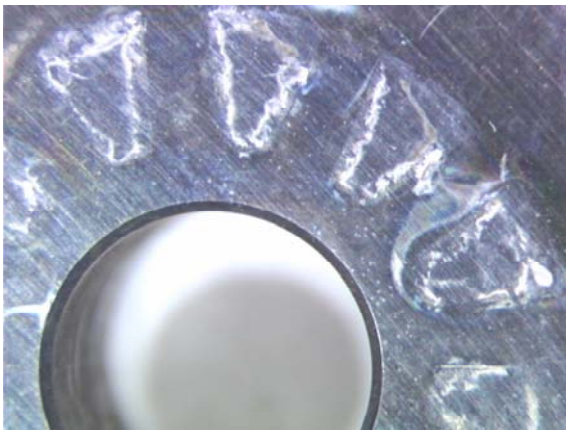

c) Specimen KE0416, non-annealed, tested in 6 m NaCl + 0.9 m KNO_3 at 100°C.

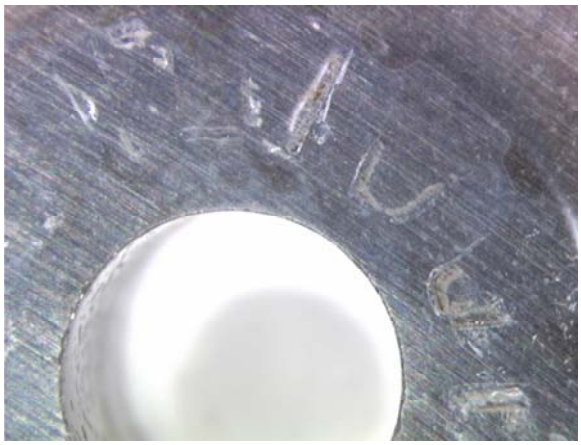

d) Specimen KE0493, solution annealed at 1300°C for 20 minutes, tested in 6 m NaCl + 0.9 m KNO_3 at 100°C.

Figure 5.4.2.3. Comparison of Welded Specimens in Non-Annealed vs. 1300°C Anneal conditions.

- In both environments, specimens show lower breakdown potentials (E_{20} and E_{crit}) with increasing annealing temperatures. This indicates that with increasing annealing temperatures, resistance to crevice breakdown tends to decrease. Specimens annealed at 1300°C, showed a significantly lower breakdown potential. Despite the higher breakdown potentials, observations show lower total area of crevice corrosion for specimens annealed at higher temperatures (Figure 5.4.2.3).

- Repassivation potentials (E_{r1} and E_{rco}) show a tendency to rise with increasing annealing temperature in 1 M NaCl at 90°C, except the E_{r1} values at 1300°C where one specimen had a much lower E_{r1} value than the other two, causing the average to be low. The same trend is observed in the 6 m NaCl + 0.9 m KNO_3 at 100°C tests, except that the specimens annealed at 1200 and 1300°C show a greater ability to repassivate crevice corrosion that has initiated. In both cases, the trend of increasing repassivation potentials indicates that samples annealed at higher temperatures are able to repassivate more easily.

5.4.3. Summary of Corrosion Testing

- While all specimens, tested in both 1 M NaCl at 90°C and 6 m NaCl + 0.9 m KNO_3 at 100°C showed localized corrosion to some degree, the specimens annealed at the highest temperatures had the lowest area of localized corrosion and qualitatively seem to have shallower crevice attack.

- Qualitatively, the specimens tested in 6 m NaCl + 0.9 m KNO_3 at 100°C also showed less localized corrosion overall than specimens tested in 1 M NaCl at 90°C. This is consistent with previous findings for wrought and welded specimens that nitrate has a beneficial effect on the localized corrosion behavior of Alloy 22.

- Overall the effects of solution annealing on Alloy 22 corrosion behavior in 6 m NaCl + 0.9 m KNO_3 at 100°C are similar to those found for 1 M NaCl:

    i. Breakdown potentials appear to be negatively impacted by annealing.
    ii. Repassivation potentials, open circuit potentials, and corrosion rates all improve with increasing annealing temperatures.
    iii. Visual observations also support that localized corrosion resistance improves with increasing solution annealing temperatures.